EXTENSION OF THE BERGSTRÖM-BOYCE MODEL TO HIGH STRAIN RATES

S. J. QUINTAVALLA,* S. H. JOHNSON

LEHIGH UNIVERSITY, DEPARTMENT OF MECHANICAL ENGINEERING AND MECHANICS
BETHLEHEM, PA, 18015

ABSTRACT

A filled polybutadiene elastomer, typical of that used in the construction of golf balls, is tested at high (> 5000s^{-1}) and low (< 0.5s^{-1}) strain rates. By using nonlinear least-squares estimation, limited to a physically realizable search domain, suitable parameters are found for the Bergström-Boyce model of time dependent finite strain elasticity. These parameters are shown to successfully represent the material behavior over this broad range of strain rates.

INTRODUCTION

Proper characterization of the impact behavior of elastomers, where the impact speed may vary, requires a constitutive model for the time- and strain- dependent behavior that works over a broad range of strain rates for the levels of strain anticipated. There are several models in recent literature which seek to describe this behavior, though rarely are such models extended to strain rates or timescales appropriate to impact (*i.e.*, millisecond or microsecond response). Models in current practice range from phenomenological nonlinear models[1,2] and applications of BKZ theory[3] to micromechanism and thermodynamic-based descriptions.[4,5] Until very recently, most of these models are tested over a very narrow range of strain rates, and often are based on the response to "step" strain over several seconds to thousands of seconds.

Wang, Arruda, and Przybylo[6] present a model showing excellent agreement over a very broad range of strain rates for plasticized poly-vinyl-chloride. The authors show that the initial "modulus" of this material at room temperature increases greatly with increasing strain rate (to a range of 5000s^{-1}), due to the proximity of the glass transition. Without the need for this wide phenomenological range (as will later be shown), with its attendant combination of material constants and adjustable parameters, this model was deemed to be extravagant.

The Bergström-Boyce model for time dependent finite strain elasticity[4,7,8] is therefore studied for several reasons. First, it uses a time-dependence that is based on micromechanical arguments, particularly the reptation theory of de Gennes[9] (given an assumption discussed under Parameter Estimation). This is important in that this model requires the identification of five parameters, all of which are material constants. Moreover, these constants are expected to be related to the composition of the material of interest. Second, examples of implementation in the literature are determined from constant strain rate load/unload experiments, which are the most easily approximated at the combinations of high strain rate and moderate strain (about 20%) of interest to this work.

EXPERIMENTAL METHODS

The material of interest is cis-(1, 4) polybutadiene. The peroxide crosslinks are formed using 25-35 phr Zinc Dimethacrylate (ZDA). Filler content typically ranges from 10-20 phr of Zinc Oxide (ZnO). The experiments described use a single proprietary blend within the above ranges. In all cases, the samples were cylindrical, with ground ends. All tests were performed at 75 °C, +/- 2°. No measurable heating of the samples was observed.

The experimental work is divided into low and high rate uniaxial compression tests. Guided

* Corresponding author. Ph: 908-470-9330; Fax: 908-234-0138; email: squintavalla@usga.org

by previous work, the low rate testing was done with samples of dimensions specified in ASTM D 6147-97,[10] on a screw driven tensile testing apparatus built by Automated Test Systems. Steel platens were used, with PTFE film to minimize frictional contact at the interfaces.[4] In addition, digital indicators were used to monitor the diametric expansion of the specimen during compression (Figure 1).

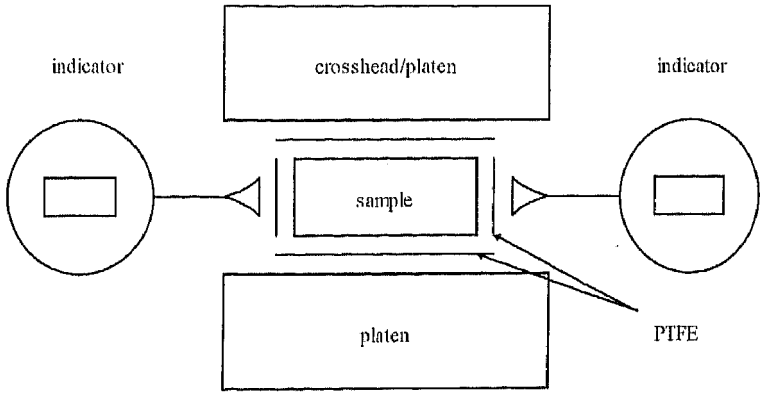

FIG. 1. — Schematic of the low-rate, screw-driven tensile apparatus for testing ASTM samples.[10] The crosshead (above) moves downward in compression, then upward during unloading. The crosshead also contains a load cell for direct force measurement. The indicators are used to measure diametric expansion, and the PTFE film is used to minimize friction between the sample surface and the steel platens.

Low strain rate tests were conducted at constant rates of 0.0003 – 0.35 s^{-1}. Owing to the nature of the screw-driven ATS apparatus, testing at the highest possible rate proved difficult to control, resulting in excess strain (-0.35 strains, versus -0.2 for all others) and a significant elapsed time between the loading and unloading. Results are shown in Figures 3 and 4.

The high-rate testing was done with a Split Hopkinson Pressure Bar[11,12] constructed specifically for this purpose, depicted in Figure 2. There are several examples of the use of SHPB testing for elastomeric materials in recent literature,[13-16] though none result in constitutive explanations of the material behavior (with the exception of the recent work of Wang,[6] *et. al.* who combined SHPB testing with the low-rate tests described above).

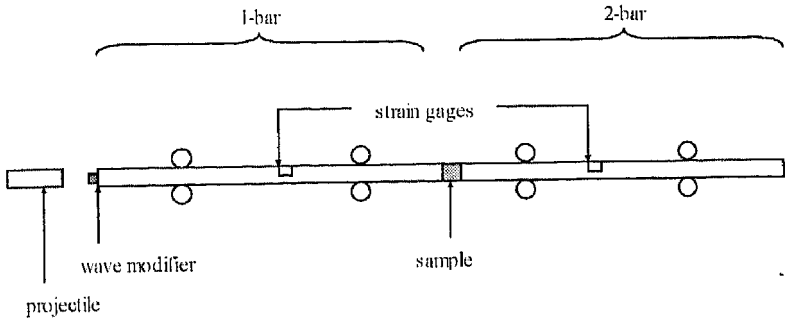

FIG. 2. — Schematic of the Split-Hopkinson Pressure Bar (SHPB). The projectile, left, strikes the wave modifier, a punched copper slug, attached to the 1-bar with a thin film of grease. The resulting (incident) strain wave travels through the 1-bar, measured by the strain gauge. Some part of the wave is reflected, due to impedance mismatch, and the remaining transmitted through the sample. Sample stress and strain may be computed

The SHPB apparatus for this study uses two 12.7 mm diameter 7075T6 aluminum rods

0.914 m in length with machined and polished ends. The rods are supported in Frelon-lined bearings in adjustable retainers. The strain gauges, 3.18 mm in gauge length with a resistance of 350Ω, are situated 0.3 m from the split. Signals are conditioned without electronic filtering through Vishay 2311 conditioners, and are read with 12 bits at 1.28 μs per sample. The resulting 2-bar stress is smoothed using a truncated Fourier series, with care that no phase-dispersed information is lost.

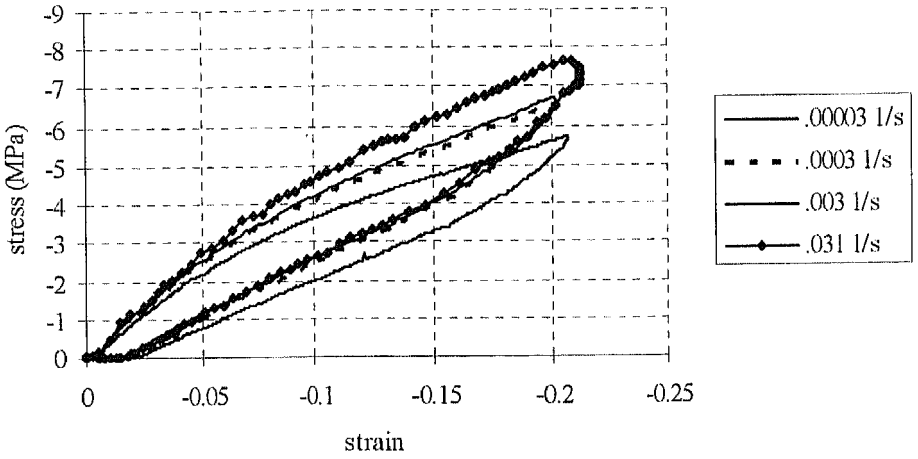

FIG. 3. — Low strain rate compression load/unload tests: Cauchy stress vs. logarithmic strain. Tests were performed using a screw-driven tensile tester, set to constant linear displacement rates.

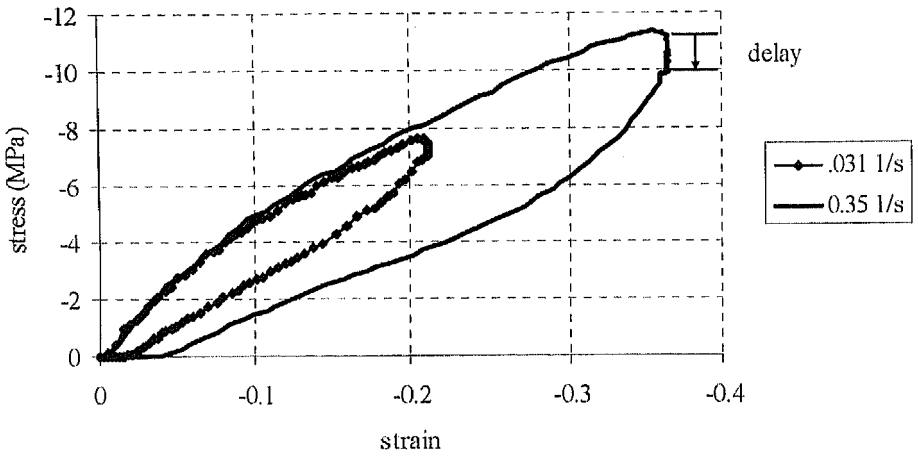

FIG. 4. — Additional low-rate stress-strain results: Cauchy stress vs. logarithmic strain, as in Figure 3. There is a significant delay during the reversal of the screw-driven mechanism.

Sample sizes range from 9.5 – 11.1 mm diameter, with thicknesses between 1.6 and 3 mm. Both diameter and thickness are chosen to achieve a desired level of strain and strain rate. Though it would be desirable to test even thicker samples, thereby investigating lower strain rates (sub-1000s^{-1}), there is an upper limit on sample thickness dictated by both the signal-to-noise ratio in the transmitted stress bar, and more importantly, the necessity of guaranteeing stress equilibrium (*i.e.*, that there are no stress waves in the sample). Samples were held in place using a thin layer of grease. In all measurements using the SHPB, the material was assumed to be

incompressible, allowing computation of Cauchy stress as a function of uniaxial strain.

While constant or near-constant strain rates are achievable using the SHPB, this inevitably comes at the price of phase dispersion in the bar itself. The result of this is an oscillatory initial straining of the sample and characteristically short pulses. The oscillation will be difficult to separate from noise, and the short pulse restricts the test envelope to one not suitable for this investigation. It is for these reasons that a strain wave modifier is used, in these experiments punched copper slugs of 2.7 mm thickness and 5 mm diameter have been found to be suitable. While the resulting strain wave is not square, and the strain rate in the sample therefore non-constant, the signal is relatively smooth. A typical resulting strain history is shown in Figure 5. The stress history associated with this is given in Figure 6, and the stress vs. strain plot is shown in Figure 7. It is important to note that the stress computed from both sides of the sample are equal, indicating that the sample is in stress equilibrium. We further show selected stress vs. strain results for 3000 – 5300 s^{-1} in Figure 8. The strain rates associated with each of the results is taken as the maximum tangential slope of strain versus time. It has been indicated from uniaxial dynamic mechanical analysis that at room temperature, the tan(δ) peak is far from the region of interest (Figure 9, by permission of Raytheon Reliability Analysis Laboratory). This is important in that it assures that a reptation-based dynamic model is appropriate for the regime of interest, and that transition effects will not play a significant role (unlike the PPVC studied by Wang, *et. al.*).[6]

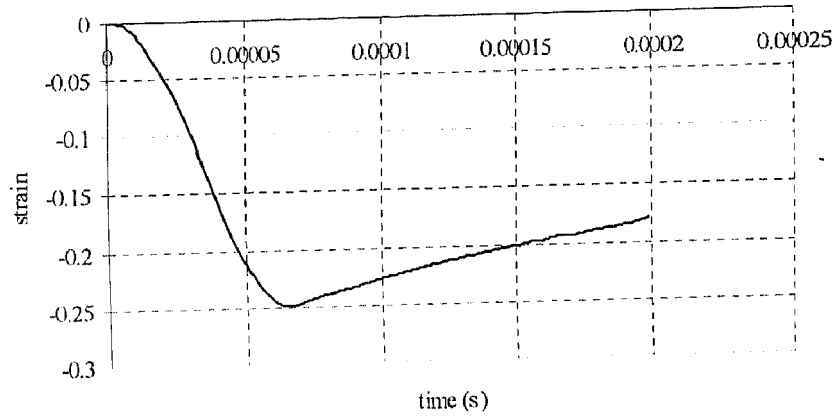

FIG. 5. — Logarithmic strain vs. time result from a typical SHPB experiment. The maximum loading rate is computed at 5332s^{-1}.

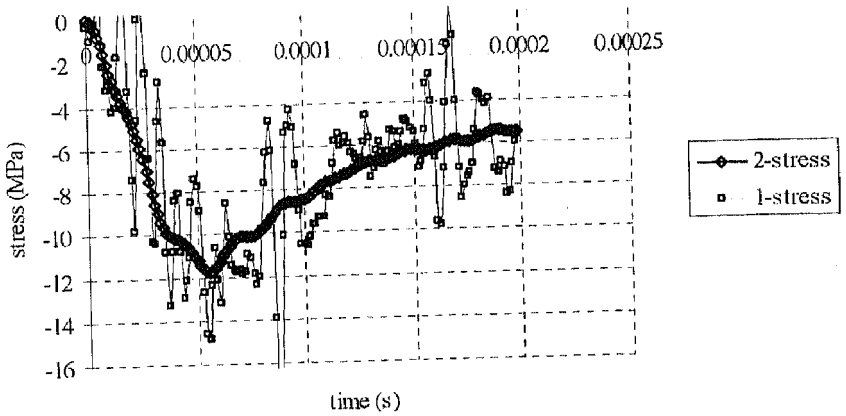

FIG. 6. — Cauchy stress vs. time result from the above experiment. The 2-stress is computed from the transmitted strain signal, and the 1-stress is computed from the difference between the incident and reflected strain signals (hence the greater noise). It is significant that the signals overlap, which indicates that the sample is dynamically in stress equilibrium.

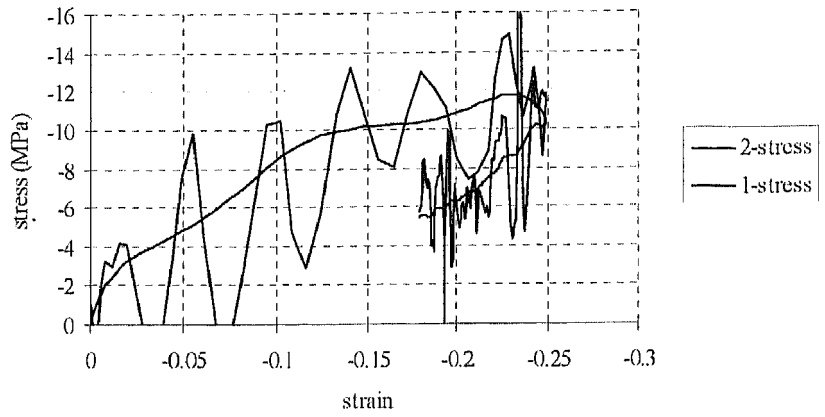

FIG. 7 — Cauchy stress vs. strain plot resulting from the 5332s^{-1} SHPB experiment, without smoothing of the 2-stress. The 1- stress is also given, as in Figure 6.

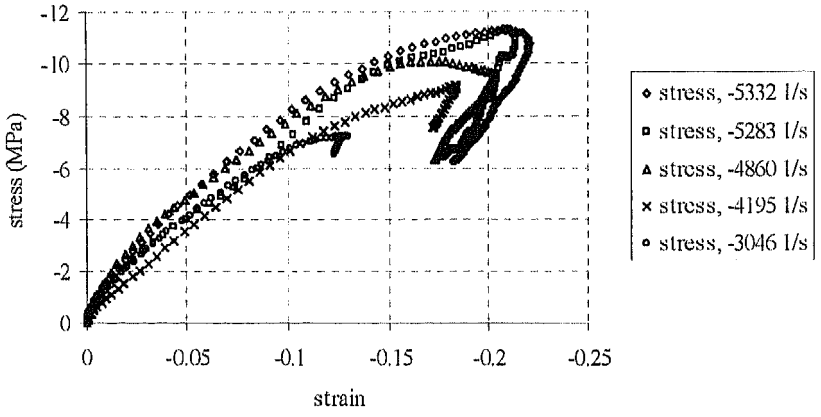

FIG. 8. — Cauchy tress vs. logarithmic strain plot for several SHPB experiments at different strain rates.

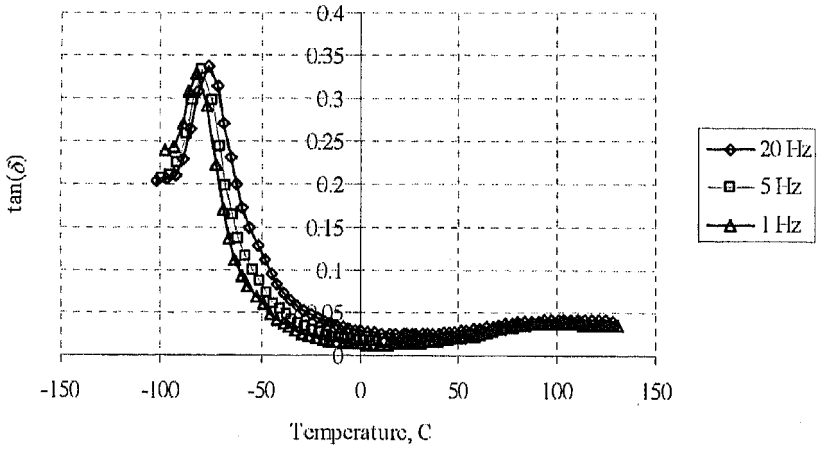

FIG. 9. — Uniaxial DMA results, published with the permission of Raytheon Reliability Analysis Laboratory. The glass transition temperature occurs at about -80 °C, indicating that transition behavior does not play a significant role at the strain rates of interest. This allows us to use a reptation-based dynamic model with confidence.

PARAMETER ESTIMATION

The Bergström-Boyce[4,7,8] model for time-dependent finite-strain elasticity is well suited as a candidate for this study, not only because of the few parameters necessary to characterize the material, but because all of the initial published work on this model was based on ramp loading and unloading, rather than stress relaxation, of elastomer specimens. As the present work seeks to identify a model for very high strain rates, *i.e.*, time scales of less than 10^{-5}s, step-strain response experiments are not appropriate. For incompressible uniaxial extension, the Bergström-Boyce model is characterized by the following equations:

$$\sigma = \sigma_A + \sigma_B \tag{1}$$

$$\sigma_A = C_A\left(\lambda^2 - \lambda^{-1}\right)\mathcal{L}^{-1}\left[\left(\frac{\lambda^2 + 2\lambda^{-1}}{3\lambda_{\lim}}\right)^{\frac{1}{2}}\right]\left(\frac{\lambda^2 + 2\lambda^{-1}}{3\lambda_{\lim}}\right)^{-\frac{1}{2}} \tag{2}$$

$$\sigma_B = C_B\left(\lambda_B^{e\,2} - \lambda_B^{e\,-1}\right)\mathcal{L}^{-1}\left[\left(\frac{\lambda_B^{e\,2} + 2\lambda_B^{e\,-1}}{3\lambda_{\lim}}\right)^{\frac{1}{2}}\right]\left(\frac{\lambda_B^{e\,2} + 2\lambda_B^{e\,-1}}{3\lambda_{\lim}}\right)^{-\frac{1}{2}} \tag{3}$$

$$\lambda_B^e = \lambda \Big/ \lambda_B^p \tag{4}$$

$$\dot{\lambda}_B^p = \sqrt{\tfrac{2}{3}}\lambda_B^p \frac{C_1}{\tau_B^{\,m}}\left[\sqrt{\tfrac{1}{3}\left(\lambda_B^{p\,2} + 2\lambda_B^{p\,-1}\right)}^{\frac{1}{2}} - 1 + \delta\right]^{-1}\left(\sqrt{\tfrac{1}{3}}\sigma_B\right)^m \tag{5}$$

where the parameters to be identified are C_A, C_B/C_A, $\lambda_{\lim}$, $\hat{C}_1 = C_1/\tau_B^{\,m}$, and m. This assumes that the exponent on the brackets in Equation 5 is fixed at -1, based on theoretical arguments. In fact, this value could range from -7 to -1, based on the work of Doi and Edwards. The value of -1 is equivalent to the assumption that deGennes-type reptation dominates the problem. This assumption is made by Bergström and Boyce successfully, and will be tested here for short timescales. Finally, the value δ, introduced more recently, is set at 0.0001, and serves to prevent singularity as λ_B^p approaches unity. This value is not determined through experimental data. Rather, it is set as low as possible while preserving numerical stability.

It is interesting to note that while the Bergström-Boyce model as published uses the Arruda-Boyce[17] finite-strain elasticity function, use of said model is not necessary to the time-dependent characterization. Though the Bergström-Boyce model is not time-strain separable in the sense of BKZ theory, the similarity in implementation of stress formulations in the proposed elastic (referred to as "A") and inelastic or viscous ("B") networks allows for some flexibility in the strain-dependent form of the model. Other forms, such as neoHookean, Mooney-Rivlin, Ogden, *etc.*[18,19] may be used within the same architecture, with appropriate modification to Equations 2 and 3. Here it is noted that given the moderate range of strains of interest in this work ($0.75 \geq \lambda \geq 1$), there is not sufficient information to identify $\lambda_{\lim}$, nor is it necessary to do so. Therefore, this parameter is fixed at a sufficiently high value (10^2) that the Arruda-Boyce model reduces to the neoHookean form, which is appropriate for this range.[20]

Marquardt-Levenberg nonlinear least squares identification[21] was used to find the non-fixed parameters for single and multiple experiments. Because of the narrow range of physical mean-

ing of some parameters, as well as the sensitivity of the Bergström-Boyce model to numerical integration for some ranges of parameters, the search domain was algebraically transformed to a finite range.

For each set of data, a large number of comparison points (typically comprising one-third to one-half of the experimental data), equally spaced in time, was chosen for computation of the penalty function χ^2, whose value was the sum of the squared errors of the comparison points. The Bergström-Boyce model was integrated forward in time using the experimental strain versus time data as a forcing function for the intermediate points, which allows for the accommodation of nonlinear stain inputs. Successful integration of the model required the use of an implicit algorithm, in this case backward Euler, using Newton's method with an iteration tolerance of 10^{-5}.

RESULTS

First, a single low-rate experiment ($0.003s^{-1}$) is fit using the four adjustable parameters (Figure 10). Next, a single high-rate experiment ($5283s^{-1}$) is fit using the same procedure (Figure 11). The agreement between the model and the experimental data is excellent, with a Pearson correlation coefficient in both cases exceeding 99%. The parameter set derived for each of these cases was applied to the other data set, with the results shown in Figure 12. Clearly, the parameter set derived from the high rate data has done a better job at fitting the low-rate experiment than the reverse. However, even in this case, the hysteresis is underestimated by nearly 50%. It seems, based on this, that the time-independent parameter C_A has been fit properly in this case, but that the time dependence has not been completely captured (note that for zero time-dependence, the result would be a fairly straight line through the middle of this loop).

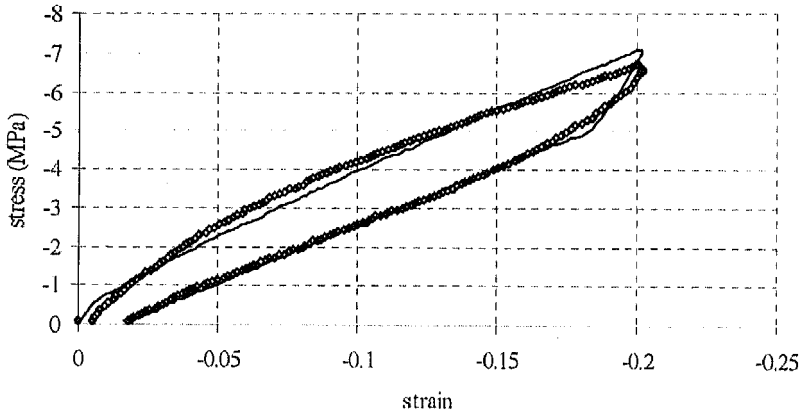

FIG. 10. — Bergström-Boyce model (solid line) applied to a low-rate ($0.003s^{-1}$) experiment. Parameter values are found in Table I.

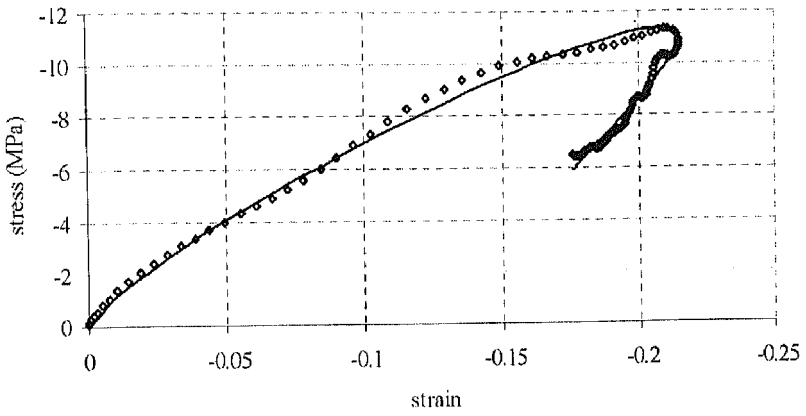

FIG. 11. — Bergström-Boyce model (solid line) applied to a high-rate ($5332s^{-1}$) experiment. Parameter values are found in Table I.

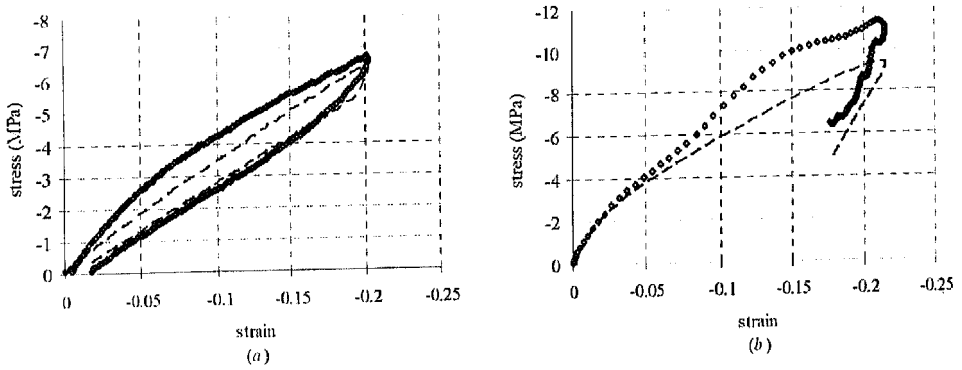

FIG. 12. — Model parameters derived from high-rate testing are applied to low rate data (*a*). The low-rate derived parameters are also applied to high-rate the high-rate data (*b*). Simulated results are given by dashed lines.

Given this limited success, parameters are then estimated using both high- and low- rate data simultaneously. This results in an $R^2 = 0.992$, and the fit is shown in Figure 13 (parameters given in Table I).

TABLE I

BERGSTRÖM-BOYCE PARAMETERS FOR SELECTED EXPERIMENTS. VALUES WERE FOUND USING LEVENBERG- MARQUARDT NONLINEAR LEAST-SQUARES IDENTIFICATION. IN ALL CASES, THE LIMITING CHAIN STRETCH WAS SET TO 10^2, EFFECTIVELY RESULTING IN A NEOHOOKEAN DESCRIPTION OF THE RUBBER ELASTICITY.

Strain rate	C_A (MPa)	C_B/C_A	C_I ($s^{-1}MPa^{-m}$)	m
0.003 s^{-1}	3.81	2.45	$2.48x10^{-1}$	10.3
5283 s^{-1}	3.64	2.68	$1.13x10^{-1}$	5.04
Multiple	3.79	2.98	$1.70x10^{-2}$	7.41

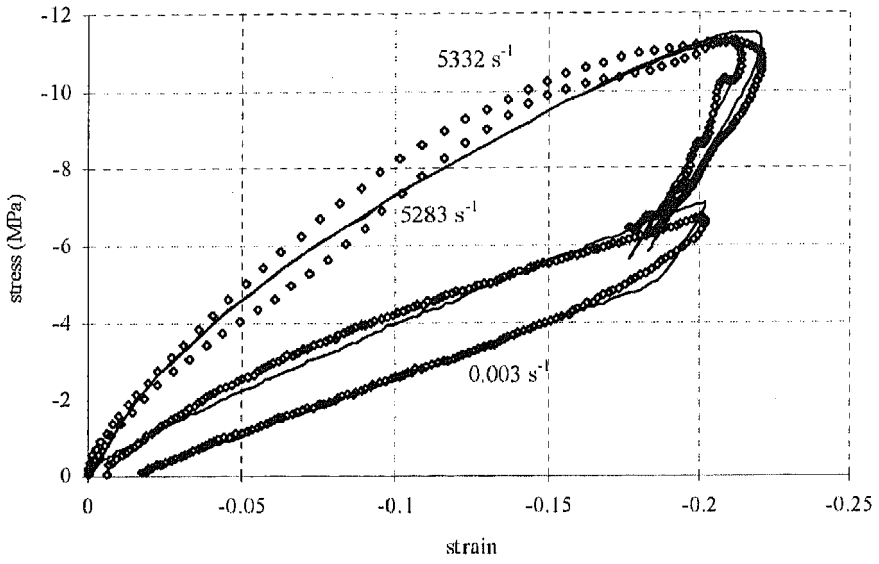

FIG. 13. — Bergström-Boyce model (solid line) applied to high- and low-rate experiments simultaneously. Parameter values are found in Table I.

Finally, in Figure 14, these parameters are used to simulate experiments at intermediate strain rates. That is, those experiments whose maximum strain rates fell between those to which the parameters were fit. Especially given that the model was not fit to these experiments, the Pearson R^2 values were very high: 0.987, 0.979, and 0.990 for $3046s^{-1}$ $0.35s^{-1}$ and $0.031s^{-1}$ experimental data, respectively. It should be noted that the least successful of these was an application where the ultimate strain was 50% higher than the experiments to which the data was fit.

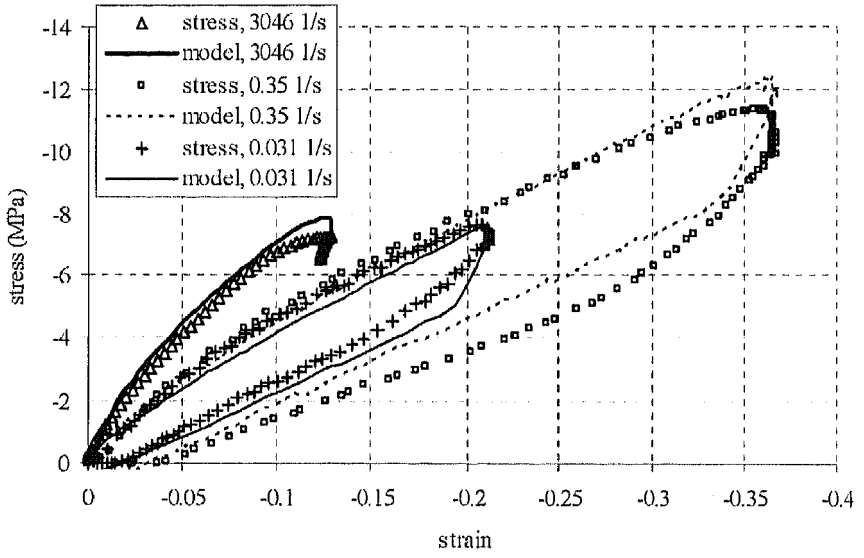

FIG. 14. — Parameters found using the experimental data in Figure 13 are applied to stress-strain results at intermediate strain rates.

CONCLUSIONS

Applicability of the Bergström-Boyce time-dependent elasticity model has been demonstrated over a range of strain rates that is much broader than previously reported. Uniaxial compression tests spanning six orders of magnitude in strain rate were shown to be successfully modeled using a single set of fitted parameters. This work did not address limiting or very large strain behavior, and it is thus left to previous literature to demonstrate the success of the Arruda-Boyce model.

It is felt that the procedure used to determine the B-B model parameters is more general than those already published. This implementation of nonlinear least-squares allows for arbitrary loading and unloading profiles and for several sets of experimental data to be fit simultaneously. The last is important in ensuring that a robust solution is found.

The following work remains: Case studies will be performed where the filler content and crosslink density will be independently varied with the same base polymer to determine the effects on the material parameters. Work will be done using uniaxial DMA at intermediate strain rates ($10^1 - 10^2\ s^{-1}$) to further demonstrate the consistency of results, though necessarily at small strains.

ACKNOWLEDGEMENTS

The authors wish to thank the United States Golf Association for financial and material support of this work.

REFERENCES

[1]A. R. Johnson and R. G. Stacer, RUBBER CHEM. TECHNOL. **66**, 567 (1993).

[2] A. R. Johnson, C. J. Quigley, and C. E. Freese, *Comput. Mthd. Appl. Mech. Eng.* **127**, 163 (1995).

[3]V. Roullier and G.B. McKenna,."A Hybrid Nonlinear Constitutive Model: Comparisons with Multiple Step Data for a Polyurethane Rubber.". in *Soc. Plast. Engin., ANTEC 98*. 1998.

[4] J. S. Bergström and M. C. Boyce, *J. Mech. Phys. Solids.* **46**, 931 (1998).

[5]A. D. Drosdov and A. Dorfmann, *Arch. Appl. Mech.* **72**, 651 (2003).

[6]Y. Wang., E. M. Arruda, and P. A. Przybylo, RUBBER CHEM. TECHNOL. **74**, 560 (2001).

[7]J. S. Bergström and M. C. Boyce, *Mech. Materials* **32**, 627 (2000).

[8]J. S. Bergström and M. C. Boyce, *Mech. Materials* **33**, 523 (2001).

[9] P. G. de Gennes, *J. Chem Phys.* **76**, 3316 (1982).

[10]ASTM. 1997, American Society for Testing and Materials: West Conshohocken.

[11]Kolsky, *Phil. Trans. R. Soc. London.* **B62** (1949).

[12]U. Lindholm, *J. Mech. Phys. Solids* **12**, 317 (1964).

[13]W. Chen, B. Zhang,. and M. J. Forrestal, *Experimental Mechanics* **38**, 8, (1998).

[14]K. Maruoka, *et al., Dynamic Impact Characteristics of Golf Ball Materials.* in *Materials and Science in Sports.* 2001: The Minerals, Metals, & Materials Society.

[15] T. Vuoristo and V.T. Kuokkala, *Mech. Materials* **34**, 493 (2002).

[16]H. Zhao, G. Gary, and J. R. Klepaczko, *Int. J. Impact Engineering* **19**, 319 (1997).

[17] E. M. Arruda and M. C. Boyce, *J. Mech. Phys. Solids* **41** (1993).

[18]M. C. Boyce and E. M. Arruda, RUBBER CHEM. TECHNOL. **73**, 504 (2000).

[19]Hibbit, Karlsson, and Sorensen, 1998, Hibbit, Karlsson, and Sorensen, Inc.: Pawtucket, RI.

[20] L.R.G. Treloar, "The Physics of Rubber Elasticity." 3 ed. Monographs on the Physics and Chemistry of Rubber. 1975, New York: Oxford, Clarendon Press.

[21]W.H. Press, *et al.*, eds. "Numerical Recipes in Fortran," 2nd Ed. 1992, Cambridge University Press: London.

[*Received March 2004, revised August 2004*]